WATER RESOURCES RESEARCH, VOL. 39, NO. 12, 1364, doi:10.1029/2003WR002554, 2003

Infiltration from surface and buried point sources: The Average wetting water content

F. J. Cook,[1,2] P. J. Thorburn,[2,3] K. L. Bristow,[2,4] and C. M. Cote[5]

Received 3 August 2003; revised 2 October 2003; accepted 8 October 2003; published 19 December 2003.

[1] The assumption in analytical solutions for flow from surface and buried point sources of an average water content, $\bar{\theta}$, behind the wetting front is examined. Some recent work has shown that this assumption fitted some field data well. Here we calculated $\bar{\theta}$ using a steady state solution based on the work by *Raats* [1971] and an exponential dependence of the diffusivity upon the water content. This is compared with a constant value of $\bar{\theta}$ calculated from an assumption of a hydraulic conductivity at the wetting front of 1 mm day^{-1} and the water content at saturation. This comparison was made for a wide range of soils. The constant $\bar{\theta}$ generally underestimated $\bar{\theta}$ at small wetted radii and overestimated $\bar{\theta}$ at large radii. The crossover point between under and overestimation changed with both soil properties and flow rate. The largest variance occurred for coarser texture soils at low-flow rates. At high-flow rates in finer-textured soils the use of a constant $\bar{\theta}$ results in underestimation of the time for the wetting front to reach a particular radius. The value of $\bar{\theta}$ is related to the time at which the wetting front reaches a given radius. In coarse-textured soils the use of a constant value of $\bar{\theta}$ can result in an error of the time when the wetting front reaches a particular radius, as large as 80% at low-flow rates and large radii. *INDEX TERMS:* 1842 Hydrology: Irrigation; 1866 Hydrology: Soil moisture; 1875 Hydrology: Unsaturated zone; *KEYWORDS:* point source, trickle irrigation, wetting patterns

Citation: Cook, F. J., P. J. Thorburn, K. L. Bristow, and C. M. Cote, Infiltration from surface and buried point sources: The Average wetting water content, *Water Resour. Res.*, *39*(12), 1364, doi:10.1029/2003WR002554, 2003.

1. Introduction

[2] Prediction of wetting patterns from trickle irrigation emitters could assist in designing the spacing and siting of trickle emitters in the soil profile. Many authors have provided methods for the prediction of wetting patterns from trickle emitters [*Bresler*, 1978; *Hachum et al.*, 1976], yet these have rarely been used in on-farm designs for trickle systems. Properly designed trickle irrigation systems can deliver highly efficient irrigation of crops [*Phene*, 1995]. However, poorly designed trickle systems can be just as inefficient in watering crops as any other system. Thus methods that can accurately predict wetting patterns from trickle emitters should help in designing efficient trickle systems.

[3] *Revol et al.* [1997a, 1997b] showed that flow from a surface point source was well described by an analytical solution. They found that analytical solutions, involving either a constant value of the water content change behind the wetting front ($\Delta\theta$) or a value of $\Delta\theta$ that varied with radius and time, both gave predictions that compared well with experimental data [*Revol et al.*, 1997b]. However, they cautioned that this might not be universally applicable. *Thorburn et al.* [2003] used this analytical solution with a constant $\Delta\theta$ to calculate wetting patterns for a range of soil types. They concluded that the wetting patterns of these soils clustered into two distinct groups, coarse soils and the rest. Here we will compare the radial wetting front position using either constant or variable $\Delta\theta$ for a range of soils.

2. Theory

[4] For soils with an exponential dependence of the hydraulic conductivity (k) upon the pressure potential (ψ), steady state flow from a buried point source can be described by [*Philip*, 1968]

$$\phi(R,Z) = \frac{\alpha Q}{8\pi\rho}\exp(Z-\rho), \quad (1)$$

and from a surface point source by [*Raats*, 1971]

$$\phi(R,Z) = \frac{\alpha Q}{4\pi}\left[\frac{1}{\rho}\exp(Z-\rho) - \exp(2Z)E_1(Z+\rho)\right], \quad (2)$$

where $\phi = \alpha.k$ is the matric flux potential [m^2 s^{-1}] with α defined by $k = k_o \exp[\alpha(\psi - \psi_o)]$, k_o is the reference hydraulic conductivity at pressure potential ψ_o, $R = \alpha r/2$, $Z = \alpha z/2$, $\rho = (R^2 + Z^2)^{1/2}$, r is the radial distance form the vertical axis [m], z is vertical distance (positive downward), Q is the source strength [m^3 s^{-1}] and $E_1(x) = \int_x^\infty \exp(-u)/u du$ is the exponential integral.

[5] To evaluate equations (1) and (2) for the soil water content $\theta(R, Z)$ requires the diffusivity as a function of θ to be known. Here we use an exponential diffusivity [*Gardner and Mayhugh*, 1958; *Brutsaert*, 1979]:

$$D(\theta) = ae^{B\theta}, \quad (3)$$

with $a = \beta\phi/[(e^\beta - 1)(\theta_s - \theta_n)\exp(\beta\theta_n/[\theta_s - \theta_n])]$, and $B = \beta/(\theta_s - \theta_n)$ where β is a parameter of the exponential

[1] CSIRO Land and Water, Brisbane, Queensland, Australia.
[2] Also at CRC for Sustainable Sugar Production, James Cook University, Townsville, Queensland, Australia.
[3] CSIRO Sustainable Ecosystems, Brisbane, Queensland, Australia.
[4] CSIRO Land and Water, Townsville, Queensland, Australia.
[5] GHD Group, Brisbane, Queensland, Australia.

0043-1397/03/2003WR002554

Table 1. Soil Physical Properties for a Range of Soils[a]

Soil Type	ε	ψ_e, m	θ_s, $m^3\,m^{-3}$	K_s, $m\,s^{-1}$	S, $m\,s^{-1/2}$	θ_n, $m^3\,m^{-3}$	$\bar{\theta}^*$, $m^3\,m^{-3}$	$\Delta\theta^*$, $m^3\,m^{-3}$	ϕ_s, $m^2\,s^{-1}$	α, m^{-1}	a, $m^2\,s^{-1}$	B
Sand	4.05	−0.121	0.395	$1.76e^{-4}$	$5.06e^{-3}$	0.133	0.281	0.148	$5.37e^{-5}$	3.28	$9.55e^{-9}$	30.5
Loamy sand	4.38	−0.09	0.41	$1.56e^{-4}$	$4.20e^{-3}$	0.140	0.297	0.157	$3.59e^{-5}$	4.46	$5.67e^{-9}$	29.6
Sandy loam	4.90	−0.218	0.435	$3.47e^{-5}$	$3.15e^{-3}$	0.199	0.334	0.135	$2.31e^{-5}$	1.50	$3.05e^{-10}$	33.9
Silt loam	5.30	−0.786	0.485	$7.20e^{-6}$	$2.83e^{-3}$	0.300	0.394	0.094	$2.39e^{-5}$	0.30	$7.92e^{-13}$	43.3
Loam	5.39	−0.478	0.451	$6.95e^{-6}$	$2.10e^{-3}$	0.257	0.367	0.110	$1.25e^{-5}$	0.56	$4.50e^{-12}$	41.1
Sandy clay loam	7.12	−0.299	0.420	$6.30e^{-6}$	$1.50e^{-3}$	0.257	0.356	0.099	$7.56e^{-6}$	0.83	$4.37e^{-13}$	48.9
Silty clay loam	7.75	−0.356	0.477	$1.70e^{-6}$	$8.93e^{-4}$	0.310	0.421	0.111	$2.63e^{-6}$	0.65	$1.47e^{-14}$	48.0
Clay loam	8.52	−0.63	0.476	$2.45e^{-6}$	$1.39e^{-3}$	0.344	0.420	0.076	$8.05e^{-6}$	0.30	$1.41e^{-16}$	60.7
Sandy clay	10.4	−0.153	0.426	$2.17e^{-6}$	$6.03e^{-4}$	0.285	0.384	0.099	$1.42e^{-6}$	1.53	$2.56e^{-15}$	56.7
Silty clay	10.4	−0.49	0.492	$1.03e^{-6}$	$7.83e^{-4}$	0.368	0.450	0.0815	$2.72e^{-6}$	0.38	$2.77e^{-18}$	64.6
Clay	11.4	−0.405	0.482	$1.28e^{-6}$	$7.72e^{-4}$	0.364	0.442	0.078	$2.78e^{-6}$	0.46	$1.27e^{-18}$	67.7

[a]After *Clapp and Hornberger* [1978]; the initial matric potential = −10 m.

diffusivity [*Reichhardt et al.*, 1972]. *Clothier and Scotter* [1982] showed that the spatial distributions $\theta(R, Z)$ and $\phi(R, Z)$ are then related by

$$\theta(R,Z) = \frac{1}{B}\ln\left\{\left[\frac{B}{a}\phi(R,Z)\right] + e^{B\theta_n}\right\}. \tag{4}$$

Philip [1984, equation (17)], assuming a constant water content $\bar{\theta}$ in the wetted volume, derived a simple expression for the relationship between the radial extent (r) of wetting, at the source, and time (t) for a surface source:

$$T(R,0) = 2\exp(R)\left(1 - R + R^2/2\right) - 2, \tag{5}$$

where

$$T = \frac{\alpha^3 Qt}{16\pi\bar{\theta}}. \tag{6}$$

Philip [1984] did not explicitly give the solution for the wetted radius from a buried source, as the streamline is curved, but this was given by *Thorburn et al.* [2003] by setting the polar angle in equation (30) of *Philip* [1984] equal to 0:

$$T(R,0) = e^R\left\{R^2 - R + \frac{1}{2}[1 - R - \ln(2)]\ln\left(2e^R - 1\right) - \frac{1}{2}L\left(2e^R\right) - \frac{\pi^2}{24}\right\}, \tag{7}$$

where L(x) denotes the dilogarithm defined by

$$L(x) = -\int_1^x \frac{\ln x}{x-1}dx. \tag{8}$$

[6] The value of a spatial constant value of $\bar{\theta}$ in equation (6) was replaced by *Revol et al.* [1997b] with

$$\Delta\theta(R) = \bar{\theta}(R) - \theta_n. \tag{9}$$

We will use a value of $\bar{\theta}$ (R) calculated by

$$\bar{\theta}(R) = \frac{1}{R^2}\left(\theta_s R_s^2 + \int_{R_s}^{R^*} R\theta(R, Z=0)dR\right), \tag{10}$$

where R_s is the dimensionless radius of the saturated region near the source, which is obtained by solving equation (1) or (2) for R_s with $\phi = \phi_s$, R^* is the radius where $\theta(R^*) = \theta_f$ and θ_f is the water content at the wetting front which is defined below. The relationship between matric flux potential at saturation, ϕ_s, and sorptivity, S [*Philip*, 1969], is [*White and Sully*, 1987]

$$\phi_s = \frac{bS^2}{(\theta_s - \theta_n)}, \tag{11}$$

where b is a parameter that varies between 1/2 and $\pi/4$, θ_s and θ_n are respectively values of the water contents at

Table 2. Soil Physical Properties for a Range of Soils With Initial Matric Potential (ψ_i) of −6 and −3 m

	ψ_i = −6 m					ψ_i = −3 m				
Soil Type	θ_n, $m^3\,m^{-3}$	$\Delta\theta^*$, $m^3\,m^{-3}$	ϕ_s, $m^2\,s^{-1}$	a, $m^2\,s^{-1}$	B	θ_n, $m^3\,m^{-3}$	$\Delta\theta^*$, $m^3\,m^{-3}$	ϕ_s, $m^2\,s^{-1}$	a, $m^2\,s^{-1}$	B
Sand (S)	0.151	0.130	$5.76e^{-5}$	$4.25e^{-9}$	32.7	0.179	0.102	$6.51e^{-5}$	$1.08e^{-9}$	37.0
Loamy sand (LS)	0.157	0.140	$3.83e^{-5}$	$2.64e^{-9}$	31.6	0.184	0.113	$4.29e^{-5}$	$7.51e^{-10}$	35.4
Sandy loam (SL)	0.221	0.113	$2.55e^{-5}$	$7.41e^{-11}$	37.4	0.255	0.079	$3.02e^{-5}$	$5.54e^{-12}$	44.4
Silt loam (SiL)	0.331	0.063	$2.86e^{-5}$	$1.53e^{-14}$	51.8	0.377	0.017	$4.07e^{-5}$	$8.32e^{-19}$	73.9
Loam (L)	0.282	0.085	$1.44e^{-5}$	$3.14e^{-13}$	47.4	0.321	0.046	$1.87e^{-5}$	$1.07e^{-15}$	61.4
Sandy clay loam (SCL)	0.276	0.080	$8.55e^{-6}$	$3.27e^{-14}$	55.4	0.304	0.052	$1.06e^{-5}$	$2.02e^{-16}$	68.9
Silty clay loam (SiCL)	0.331	0.090	$3.01e^{-6}$	$6.08e^{-16}$	54.9	0.362	0.058	$3.82e^{-6}$	$9.47e^{-19}$	69.8
Clay loam (CL)	0.365	0.055	$9.60e^{-6}$	$6.57e^{-19}$	72.3	0.396	0.024	$1.33e^{-5}$	$2.34e^{-24}$	100.4
Sandy clay (SC)	0.299	0.085	$1.58e^{-6}$	$1.84e^{-16}$	63.2	0.320	0.064	$1.89e^{-6}$	$1.55e^{-18}$	75.5
Silty clay (SiC)	0.387	0.063	$3.20e^{-6}$	$1.21e^{-20}$	76.0	0.413	0.037	$4.28e^{-6}$	$8.13e^{-26}$	101.7
Clay (C)	0.380	0.062	$3.23e^{-6}$	$6.94e^{-21}$	78.8	0.404	0.038	$4.22e^{-6}$	$1.18e^{-25}$	103.0

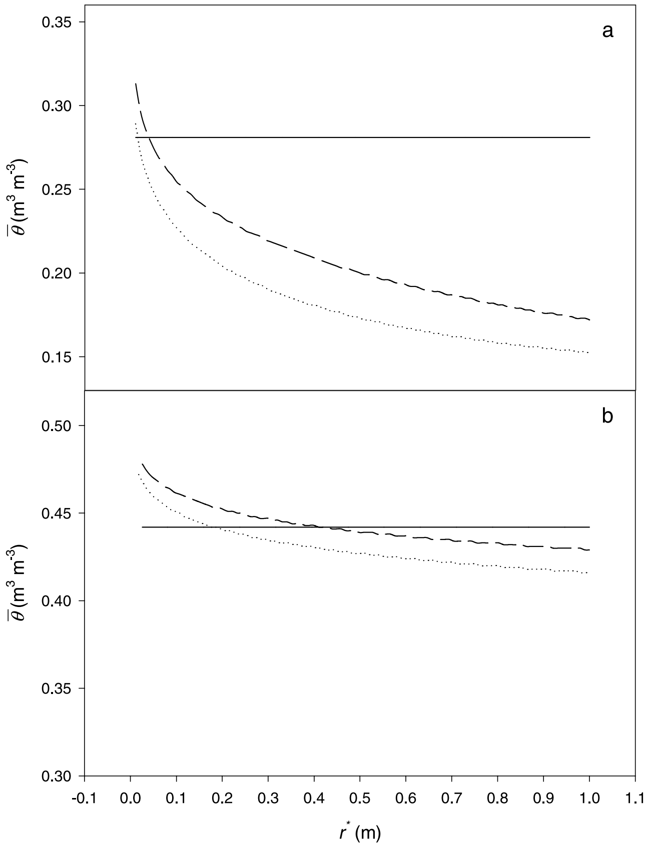

Figure 1. Change in $\bar{\theta}$ with r^* compared with $\bar{\theta}^*$ (solid line) for surface (dashed line) and buried (dotted line) sources with Q 1 L h^{-1}; a) sand and b) clay.

saturation and initially [m^3 m^{-3}]. Note that in the work of *Revol et al.* [1997a, 1997b], *B* and *b* in equations (3) and (11) were given the same symbol, implying they were equal. This is an error [B.E. Clothier, personal communication, 2002].

3. Methods

[7] *Clapp and Hornberger* [1978] presented a list of soil properties related to the texture of soils. These data are used in an earlier study [*Thorburn et al.*, 2003], and the same data set will be used here. Some of the properties needed in the calculations were derived from Clapp and Hornberger's data in the following manner. The data does not explicitly give values of ϕ_s but these can be calculated from the sorptivity, S [m s$^{-1/2}$], using equation (11) with b = 0.55 [*White and Sully*, 1987]. The initial constant water content θ_n prior to irrigation, was calculated for a matric potential ψ of -10 m, using the *Brooks and Corey* [1966] functional relationship:

$$\frac{\theta}{\theta_s} = \left(\frac{\psi}{\psi_\varepsilon}\right)^{\varepsilon}, \tag{12}$$

where ψ_e is the air-entry potential [m] and ε is an empirical constant. The constant average water content, $\bar{\theta}^*$, was calculated by

$$\bar{\theta}^* = \frac{\theta_s + \theta_f}{2}, \tag{13}$$

where θ_f is the water content at the wetting front. The value of θ_f was calculated as the value of θ when the hydraulic conductivity K_f is 1 mm day^{-1}, this is an arbitrary choice which was found to match with numerical results particularly for finer-textured soils [*Cook et al.*, 2003a], using (after *Clapp and Hornberger* [1978])

$$\theta_f = \theta_s\left(\frac{K_f}{K_s}\right)^{1/(2\varepsilon-3)}, \tag{14}$$

where K_s is the hydraulic conductivity [m s^{-1}] at saturation. The time constant $\Delta\theta$, is $\Delta\theta^* = \bar{\theta}^* - \theta_n$. From equations (6), (7) and (8) it follows that T is only dependent on R in equations (6) and (8). Hence T will have the same value for both $\Delta\theta$ and $\Delta\theta^*$ at the same value of R and hence

$$\tau = \frac{t}{t^*} = \frac{\Delta\theta^*}{\Delta\theta}, \tag{15}$$

where t and t^* are the time for the wetting front to reach the same radius, $r^* = 2R^*/\alpha$, for $\Delta\theta$ and $\Delta\theta^*$ respectively. This implies that when $\tau > 1$ it takes longer for the wetting front to reach a particular radius using $\Delta\theta$ than would be predicted using $\Delta\theta^*$ and *vice versa* for $\tau < 1$. If we consider the true value to be given using $\Delta\theta$, then the error due to using $\Delta\theta^*$ is described by the magnitude of τ at a particular value of r^*. The total error over the range of r^* is given by the root mean square of the difference (RSME):

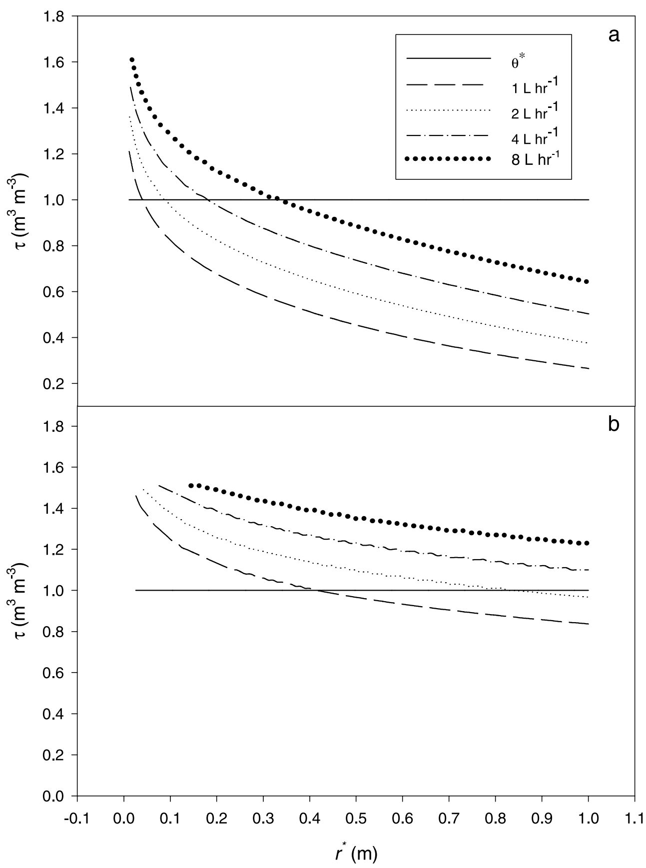

Figure 2. Relationship between τ and r^* for a surface source with various flow rates: (a) sand and (b) clay.

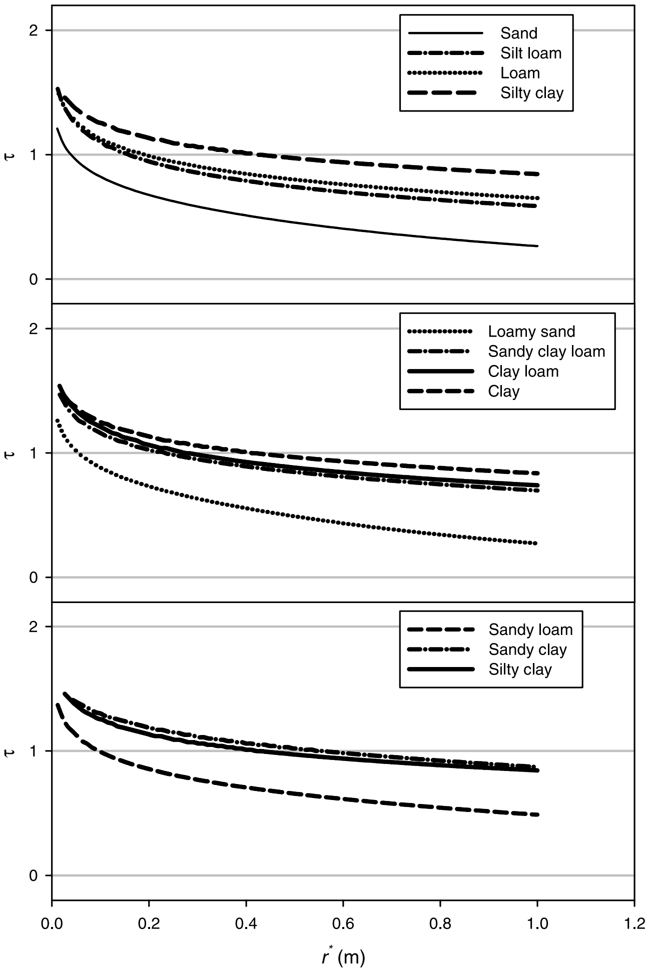

Figure 3. Relationship between τ and r^* for a surface source for all soil types in Table 1 at a flow rate of 1 L h^{-1}.

$$\mathrm{RSME} = \sum_{i=1}^{100} [\tau(r_i^*) - 1]^2, \qquad (16)$$

where $r_i^* = r_s + \Delta r$, r_s is the saturated radius calculated with either equation (1) or (2), $\Delta r = (r_m - r_s)/100$ and r_m is the maximum radius taken here as 1 m.

[8] The parameters a, B were calculated assuming $\beta = 8$ [*Reichardt et al.*, 1972; *Brutsaert*, 1979; *Revol et al.*, 1997a]. The parameters used in the calculation are listed in Table 1. The calculation procedure consisted of firstly solving either equation (1) or (2) to obtain r_s. Then $\bar{\theta}$, $\Delta\theta$ and τ were calculated for $r_s < r^* < 1$ m, for values of Q of 1, 2, 4 and 8 L hr^{-1}. This required sequentially solving equations (4), (10), (9), (6), and (15). The effect of initial water content on these calculations was evaluated by calculating the water content at two additional initial matric potential values, namely, −6 m and −3 m, using equation (12). This results in some of the other parameters changing and these values are listed in Table 2.

4. Results

[9] The results show a general trend with $\bar{\theta}$ (r^*) being under-predicted by the temporally constant value of $\bar{\theta}^*$ at small values of r^* and over-predicted at large values of r^* (Figure 1). The radius at which the change occurs from under- to over-prediction is greater for the surface source than the buried source (Figure 1). For sand the overestimate of $\bar{\theta}(r^*)$ by $\bar{\theta}^*$ occurs for all except small values of r^*. As Q increases so does the value of r^* at which this crossover occurs (Figure 2). The starting radius at which the values of τ are plotted in Figure 2 is $r_s + \Delta r$. The flow rate has little effect on $r_s + \Delta r$ for the sand but a marked effect for the clay (Figure 2) due to the increase in r_s. The value of τ, at a specific radius, increases with flow rate for both soils with generally $\tau > 1$ at low values of r^* and $\tau < 1$ and high values of r^* except at the two highest flow rates for the clay where $\tau > 1$ for the range of r^* shown (Figure 2).

[10] The range in τ for a flow rate of 1 L hr^{-1} shows that the coarser textured soils (sand, loamy sand and sandy loam) generally have values of τ less than the finer-textured soils at the same radius (Figure 3) and overall have a larger RMSE (Figure 4a). However, as the flow rate increases, the RMSE for the coarser textured soils decreases and at a flow rate of 8 L hr^{-1} these soils have the lowest RMSE (Figure 4d). This is due to the effect shown in Figure 2b where for the clay soil, at high-flow rates, $\tau > 1$ for the whole range of r^*.

[11] The effects of initial water content on τ are only shown for sand and clay soils to show the contrast in results. The relative effect of the initial matric potential on the value of τ is greater for the clay than the sand (Figure 5). The relationship between τ and r^* for the sand, for all initial matric potentials and both buried and surface sources, are similar (Figures 5c and 5d). The different response to initial matric potential of clay compared with sand, is only partly explained by the relative change in $\Delta\theta^*$ for the two soils. For clay $\Delta\theta^*$ reduces by 25 and 50% respectively, while for sand the reduction is 12 and 31% respectively as the initial matric potential increases from −10 to −6 and −3 m. Thus the relative change in $\Delta\theta^*$ for the sand when the initial matric potential increases from −10 to −3 m is > for the clay when the initial matric potential increases from −10 to −6 m, yet the shift in relationship between τ and r^* for the sand is < for the clay.

5. Discussion

[12] *Revol et al.* [1997b] obtained similar predictions of the wetted radius using either $\Delta\theta$ and or $\Delta\theta^*$, and both compared well with field measurements. Figure 4 of *Revol et al.* [1997a] shows that there was little change in water content as a function of r at various times. This lack of variation in water content with r will have contributed to their good predictions of the radial wetting obtained using $\Delta\theta^*$. Results presented here would suggest that their results are due to a combination of the properties of the soil and the flow rate in their study.

[13] For a wide range of soils at low- to moderate-flow rates and with properties in the range of the finer soils in Table 1, $\Delta\theta^*$ gives good predictions of wetting front positions. Even in coarse soils, only low-flow rates and long infiltration times give predictions of r^* that are substantially different for $\Delta\theta^*$ compared with $\Delta\theta$. This can be illustrated by using an example from *Thorburn et al.* [2003]. They predict that after 24 hours of irrigation at the flow rate of 1.65 L hr^{-1} the predicted radius is 0.42 m in

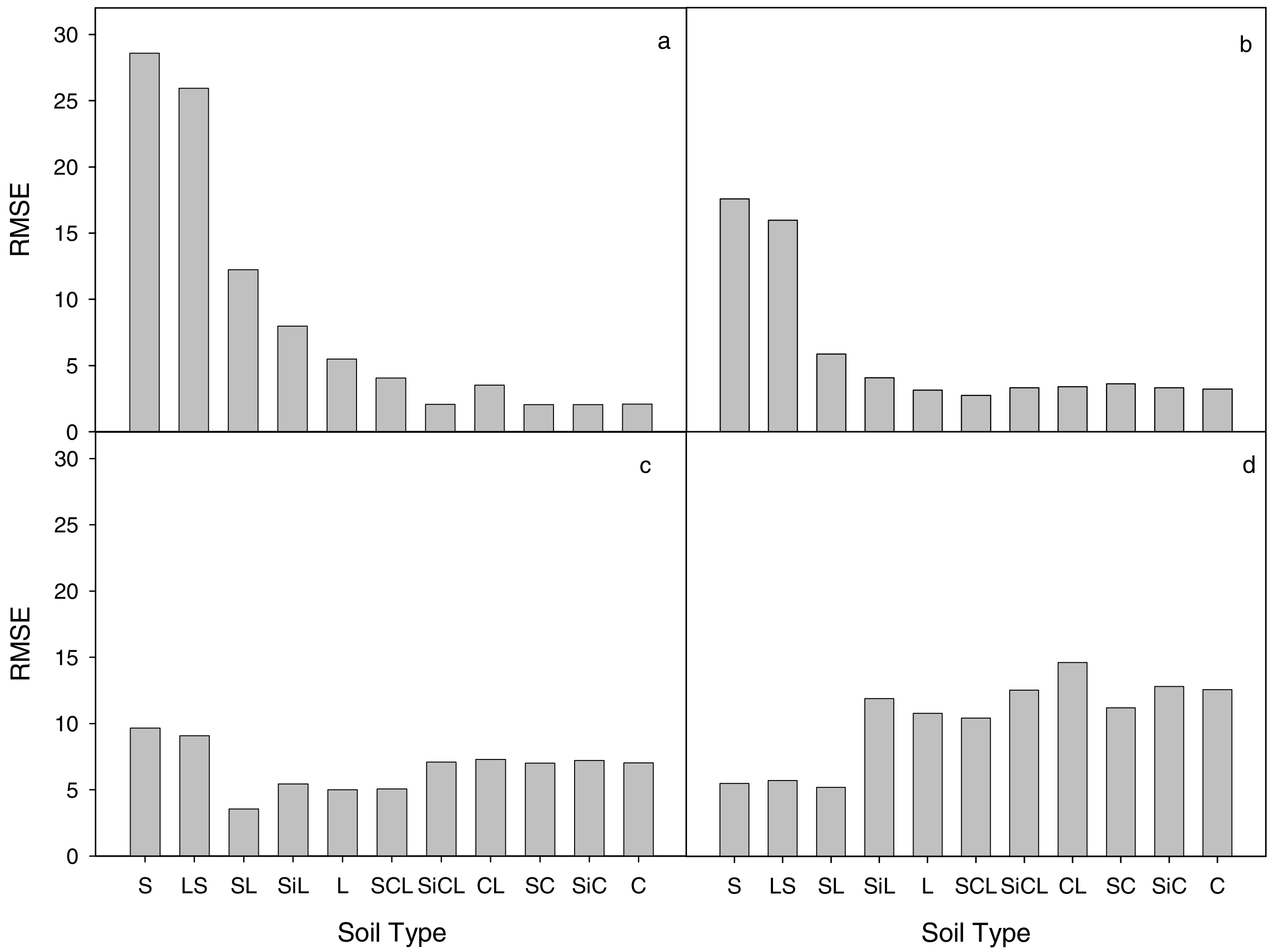

Figure 4. RSME for each soil type (see Table 2 for symbol related to soil type) for flow rates of (a) 1 L hr^{-1}, (b) 2 L hr^{-1}, (c) 4 L hr^{-1}, and (d) 8 L hr^{-1}.

the sand. From Figure 2 the value of τ, at this value of r^*, is approximately 0.6. This implies that if *Thorburn et al.* [2003] had used $\Delta\theta$ instead of $\Delta\theta^*$ they would have predicted the arrival of the wetting front about 10 hours earlier. The radius predicted at 24 hours when $\Delta\theta$ is used is approximately 0.5 m, which represents a 25% increase in r^*. *Revol et al.* [1997b, Figure 4] showed variability in measured wetted radius of approximately 30%. Given the variability in soil properties 25% error in estimating r^* using $\Delta\theta^*$ may be acceptable. For a clay, *Thorburn et al.* [2003] calculated r^* to be 0.6 m after 24 hours of infiltration. Again from Figure 2 it can be deduced that τ is approximately 1, so the radius would be well predicted using $\Delta\theta^*$.

[14] For likely application volumes (*Q.t*), the range of r^* presented here is sufficient for most practical purposes. Given the results presented in Figures 3 and 4 and examples given above it is likely that errors in predicting r^*, when $\Delta\theta^*$ is used, will be generally less than 25%. This means that the conclusions of *Thorburn et al.* [2003] based on calculations using $\Delta\theta$ are valid and the model presented by *Cook et al.* [2003b] should be useful in assisting in the design of irrigation systems. However, there may still be a considerable error in the volume of soil wetted during the irrigation caused by errors in estimation of radius.

[15] The relative lack of effect of initial water content on τ for sand, indicates that for coarser soils the choice of initial water content will not greatly change the error due to using $\Delta\theta^*$. The parallel nature of the curves in Figure 3 for clay shows that value of the initial matric potential (ψ_i) shifts the $\tau(r^*)$ relationship on the τ axis but the range in τ is similar. For finer-textured soils as ψ_i increases, the use of $\Delta\theta^*$, is likely to result in the overestimation of r^* at a particular time, especially for small values of time.

6. Conclusions

[16] These results suggest that the use of a constant average water content behind the wetting front when predicting wetting patterns from point sources using the solutions of *Philip* [1984] will give a good approximation of the wetting front position for most soils but is likely to underestimate the extent of wetting in sands at low-flow rates and overestimate the extent of wetting in clay soils at high-flow rates.

[17] The approach taken here and by *Thorburn et al.* [2003] in calculating $\Delta\theta^*$ gives reasonable results, when used to calculate wetting front positions, given the variabil-

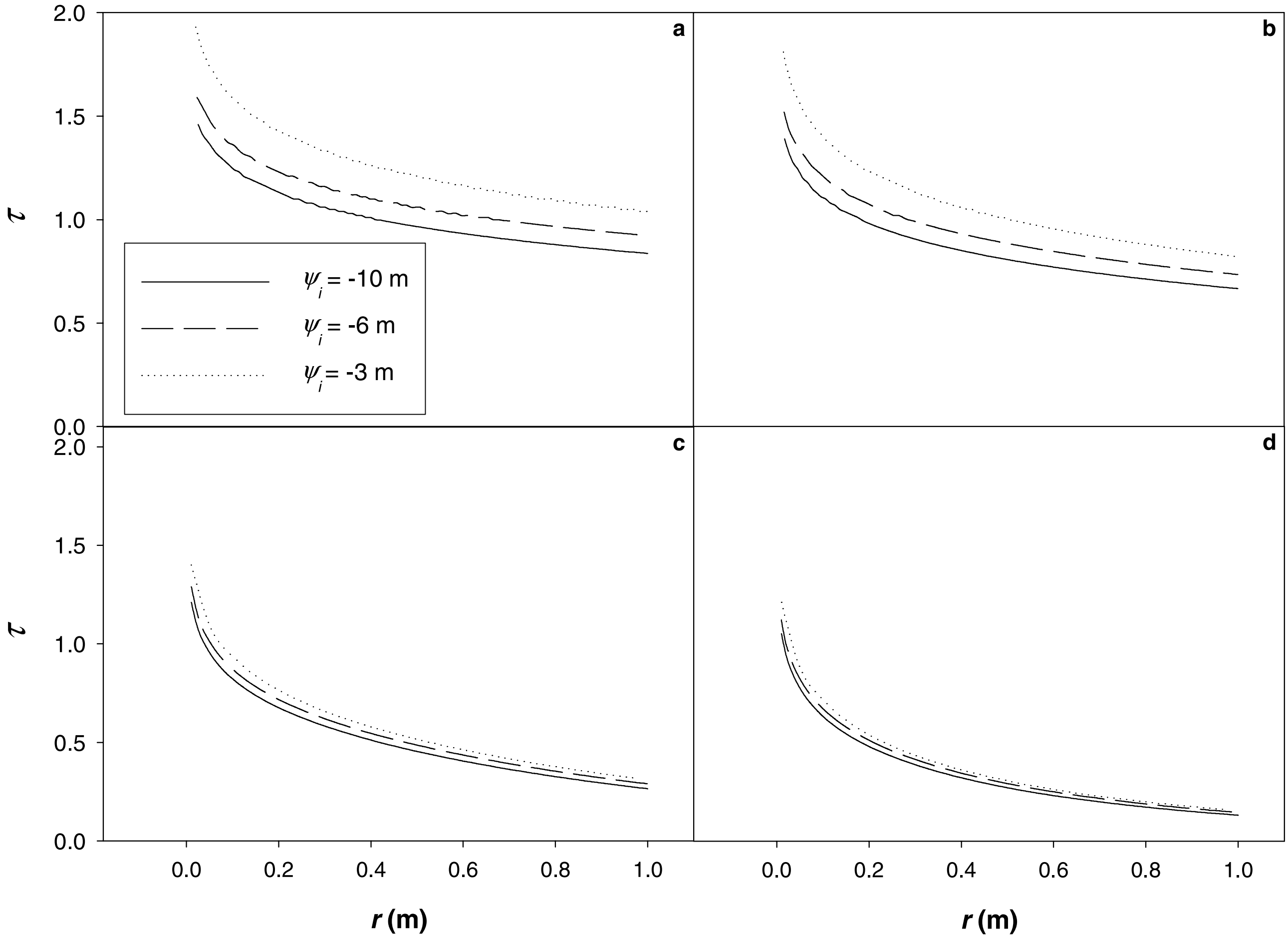

Figure 5. Relationship between τ and r^* at different initial water contents calculated using initial matric potentials shown in the legend at a flow rate of 1 L h^{-1} for (a) clay soil with a surface source, (b) clay soil and buried source, (c) sand soil and surface source, and (d) sand soil and buried source.

ity found in soil properties. In soils with coarser texture or properties similar to the coarser textured soils in Table 1 at low-flow rates and long irrigation times, or finer-textured soils at high-flow rates and short irrigation times a variable water content proposed by *Revol et al.* [1997b] will provide better predictions of the radial extent of wetting from a point source.

[18] **Acknowledgments.** The authors would like to acknowledge the suggestions for improvements in the manuscript by Paul Hutchinson and Mat Gilfedder. This work was supported in part by CSIRO, the CRC for Sustainable Sugar Production, and the Land and Water Australia National Program on Irrigation Research and Development (NPIRD).

References

Bresler, E., Analysis of trickle irrigation with application to design problems, *Irrig. Sci.*, *1*, 3–17, 1978.
Brooks, R. H., and A. T. Corey, Properties of porous media affecting fluid flow, *Proc. Irrig. Drainage Div. Am. Soc. Civ. Eng.*, *92*, 61–88, 1966.
Brutsaert, W., Universal constants for scaling the exponential soil water diffusivity?, *Water Resour. Res.*, *15*, 481–483, 1979.
Clapp, R. B., and G. M. Hornberger, Empirical equations for soil hydraulic properties, *Water Resour. Res.*, *14*, 601–604, 1978.
Clothier, B. E., and D. R. Scotter, Constant-flux infiltration from a hemispherical cavity, *Soil Sci. Soc. Am. Proc.*, *46*, 696–700, 1982.
Cook, F. J., P. Fitch, P. Thorburn, P. B. Charlesworth, and K. L. Bristow, Modelling trickle irrigation: Comparison of analytical and numerical models for estimation of wetting front position with time, in *MODSIM 2003, Proceedings of the International Congress on Modelling and Simulation, Townsville, Australia, 13–17 July 2003*, edited by D. A. Post, pp. 212–217, Modell. and Simul. Soc. Aust. and N. Z., Brisbane, Queensland, Australia, 2003a.
Cook, F. J., P. J. Thorburn, P. Fitch, and K. L. Bristow, WetUp, a software tool to approximate wetting patterns from drippers, *Irrig. Sci.*, *22*, 129–134, doi:10.1007/s00271-003-0078-2, 2003b.
Gardner, W. R., and M. S. Mayhugh, Solutions and test of the diffusivity equation for the movement of water in soil, *Soil Sci. Soc. Am. Proc.*, *22*, 197–201, 1958.
Hachum, A. Y., J. F. Alfaro, and L. S. Willardson, Water movement in soil from a trickle source, *Proc. Irrig. Drainage Div. Am. Soc. Civil Eng.*, *102*, 179–192, 1976.
Phene, C. J., Research trends in microirrigation, in *Microirrigation for a Changing World: Conserving Resources/Preserving the Environment, Proceedings of the Fifth International Microirrigation Congress, Orlando, Florida, USA, 2–6 April 1995*, edited by F. R. Lamm, pp. 6–24, Am. Soc. of Agric. Eng., St. Joseph, Mich., 1995.
Philip, J. R., Steady infiltration from buried point sources and spherical cavities, *Water Resour. Res.*, *4*, 1039–1047, 1968.
Philip, J. R., Theory of infiltration, *Adv. Hyrosci.*, *5*, 215–296, 1969.
Philip, J. R., Travel times from buried and surface infiltration point sources, *Water Resour. Res.*, *20*, 990–994, 1984.
Raats, P. A. C., Steady Infiltration from point sources, cavities and basins, *Soil Sci. Soc. Am. Proc.*, *35*, 689–694, 1971.

Reichhardt, K., D. R. Nielsen, and J. W. Biggar, Scaling of horizontal infiltration into homogeneous soils, *Soil Sci. Soc. Am. Proc.*, *36*, 241–245, 1972.

Revol, P., M. Vauclin, G. Vachaud, and B. E. Clothier, Infiltration from a surface point source and drip irrigation: 1. The midpoint soil water pressure, *Water Resour. Res.*, *33*, 1861–1867, 1997a.

Revol, P., B. E. Clothier, J.-C. Mailhol, G. Vachaud, and M. Vauclin, Infiltration from a surface point source and drip irrigation: 2. An approximate time-dependent solution, *Water Resour. Res.*, *33*, 1869–1874, 1997b.

Thorburn, P. J., F. J. Cook, and K. L. Bristow, Soil-dependent wetting from trickle emitters: Implications for system design and management, *Irrig. Sci.*, *22*, 121–127, doi:10.1007/s00271-003-0077-3, 2003.

White, I., and M. J. Sully, Macroscopic and microscopic capillary length and timescales from field infiltration, *Water Resour. Res.*, *23*, 1514–1522, 1987.

K. L. Bristow, CSIRO Land and Water, Davis Laboratory, PMB Aitkenvale, QLD 4814, Australia.

F. J. Cook, CSIRO Land and Water, 120 Meiers Road, Indooroopilly, QLD 4068, Australia. (freeman.cook@csiro.au)

C. M. Cote, GHD Group, 201 Charlotte St., Brisbane, QLD 4000, Australia.

P. J. Thorburn, CSIRO Sustainable Ecosystems, 306 Carmody Road, St. Lucia, QLD 4067, Australia.